This is an open access article published under an ACS AuthorChoice License, which permits copying and redistribution of the article or any adaptations for non-commercial purposes.

THE JOURNAL OF PHYSICAL CHEMISTRY B

Article

pubs.acs.org/JPCB

Water Effect on Acid-Gas Capture Using Choline Lactate: A DFT Insight beyond Molecule−Molecule Pair Simulations

Gregorio García,[†] Mert Atilhan,*[,‡] and Santiago Aparicio*[,†]

[†]Department of Chemistry, University of Burgos, 09001 Burgos, Spain

[‡]Department of Chemical Engineering, Qatar University, P.O. Box 2713, Doha, Qatar

Supporting Information

ABSTRACT: The suitability of CO_2 and SO_2 capture by using choline lactate ionic liquid as a sorbent and the effect of water content for acid-gas absorption were investigated through density functional theory (DFT) simulations in this work. Simulations that contain model systems considering up to four molecules (cholinium, lactate, water, and CO_2/SO_2) have been analyzed, and compositional effects on small cluster(s) formed by four ionic pairs and variable number of water molecules have been studied in this work. Assessment of the effect of water content on acid-gas capture that uses exotic ionic liquids is a rare study, and our results showed that water presence hinders CO_2/SO_2 affinity and solubility dramatically, mainly due to the dominated affinity between the ionic pair and water molecule rather than the CO_2/SO_2 molecule. Moreover, our studies also showed that affinity between ionic liquid and CO_2 is hindered by more than ionic liquid and SO_2 rich system with the presence of water in the environment.

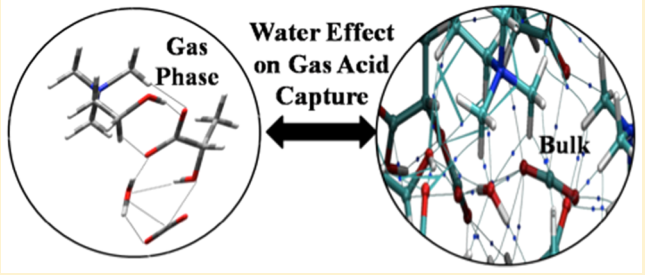

1. INTRODUCTION

Ionic Liquids (ILs) are attracting great attention due to their potential applications for a diverse range of technological applications and chemical process such as separation, organic synthesis, catalysis, electrochemistry, functional materials, and so forth.[1,2] ILs are low melting salts, which are composed by an organic cation and inorganic or organic anion, which exhibit unique properties such as good thermal properties, improved chemical stability, nonflammability, and more interestingly almost null vapor pressure. All these features have been proved to be useful in chemical processes to replace problematic volatile organic compounds in various chemical process and mechanical applications.[1,2] One of the most relevant applications of ILs is their use as promising candidates for carbon dioxide (CO_2) absorption and separation,[2−4] which has led to a large number of studies focusing mostly on imidazolium, pyridinium, or guanidinium based cations paired with various different anions such as fluorinated or acetate based anions.[4−7] Probably the most relevant feature of ILs is that they can be considered as task-specific compounds, and thus, suitable anion/cation combinations may be designed by considering the plethora of available ions in order to fulfill the complicated chemical process requirements. Nevertheless, the design of ILs with improved or selected features for a targeted applications (e.g., CO_2 capture) requires a deep knowledge about factors governing the physical and chemical background of the process as well as their relationship with the molecular structure. However, the large number of possible cation−anion combinations hinders to carry out systematic experimental screening studies due to the time and economic constraints. This is a typical context wherein molecular simulations are a powerful tool to obtain better insights into the mechanism acquiring desired properties such as absorption, which in turn provides guidance for experimental studies. Such studies allow us to improve the existing structure−property relationships and develop new state-of-the-art solutions to target specific applications.[8−12] Some types of ILs are highly hygroscopic compounds and absorbed water has a strong effect on ILs properties.[13] The possibility of using completely dried ILs for CO_2 capture purposes is not economically feasible by considering the large amounts of required ILs and the associated costs with it. Therefore, the molecular structure of ILs and its interactions with CO_2 and water content plays an important role on the efficiency of CO_2 capture.[14] As matter of fact, for imidazolium based ILs, it is reported that water effect decreases the CO_2 solubility.[15] Moreover, there are other works about water effects on the CO_2 capture through molecular dynamic simulations.[12,16,17] Apart from CO_2 capture agents, ILs are also promising candidates for SO_2 absorption. In this sense, several experimental studies on SO_2 capture by ILs have recently appeared;[18,19] however, theoretical studies on SO_2 capture mechanism by using simulation tools are scarce when compared similar studies conducted on CO_2 capture.[19,20] As concerns as water effects on acid gas (CO_2 and SO_2) capture by using ILs, most of the available literature is based on molecular dynamic simulations, which also allows a realistic approach to

Received: January 8, 2015
Revised: April 9, 2015
Published: April 13, 2015

© 2015 American Chemical Society

DOI: 10.1021/acs.jpcb.5b00184
J. Phys. Chem. B 2015, 119, 5546−5557

macroscopic properties with industrial relevance such as density, viscosity, or diffusion coefficients.[7,8,10,12,16,17,21] Meanwhile, the use of density functional theory (DFT) method is limited to the study of interactions between molecular pairs, for example, cation−anion, ion−CO_2, or ion−H_2O in gas-phase.[11,22] Other approximations, such as COSMO-RS[23] (Conductor-like Screening Model for Real solvent), have also been applied to predict CO_2 solubility in ILs from quantum chemistry calculations of individual molecules.[6,24]

Previously, we have analyzed the properties of choline lactate ([CH][LAC]) (Figure 1) and its application for CO_2 absorption using computational tools.[8,21] [CH][LAC] IL has been identified as suitable for CO_2 capture due to (i) its suitable environmental, toxicological and low cost properties and (ii) the presence of functional groups (such as hydroxyl and carboxylate) in their molecules, which could lead to complex interactions both between the involved ions, CO_2/SO_2, and water molecules.[25,26] We studied and analyzed CO_2 absorption from the molecular point of view through the combination of DFT simulations, COSMO-RS approximation to predict gas solubility and molecular dynamics simulations and concluded with exhibiting an accurate knowledge on [CH][LAC] IL and its suitability as CO_2 capture agent.[8] Despite strong interactions between the cation and the gas molecule with the presence of OH groups, they might still hinder the CO_2 capture performance.[25,26] On the other hand, the analysis of structural and dynamic parameters showed that the addition of water does not disturb the fluid's structuring but lead to strong water−ion interactions, which obstructed CO_2 capture.[21] Both works provide a detailed analysis on the suitability of CO_2 capture by [CH][LAC] IL.

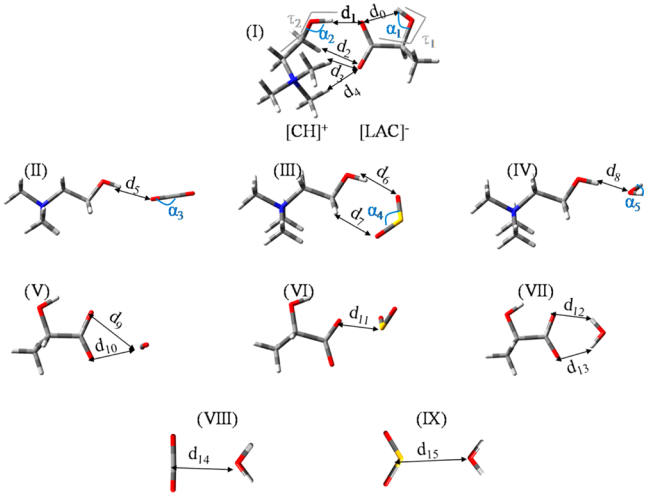

Figure 1. Molecular structure for optimized pairs optimized at the B3LYP/6-31+G** level along main optimized structure parameters: (I) IL, (II) [CH]−CO_2, (III) [CH]−SO_2, (IV) [CH]−H_2O, (V) [LAC]−CO_2, (VI) [LAC]−SO_2, (VII) [LAC]−H_2O, (VIII) CO_2−H_2O, and (IX) SO_2−H_2O. Atom color code: (gray) carbon, (red) oxygen, (yellow) sulfur, (blue) nitrogen, and (light gray) hydrogen.

To complement our previous work in which the suitability of [CH][LAC] IL for CO_2 capture as well as the effect of water to this process reported, SO_2 capture has been investigated. A DFT study was conducted on the effect of water on the interactions between both CO_2 and SO_2 acid gases and [CH][LAC] IL, which is a very relevant feature considering the highly hygroscopic character of [CH][LAC] IL.[27] The objective of this work is to analyze the suitability of [CH][LAC] IL as SO_2 capture agent and the effect of water on this process. This work will allow development of useful structure−property relationships for the rational design of ILs.

2. COMPUTATIONAL DETAILS

In the case of [CH][LAC] IL, the CO_2 capture is a physical process determined by the intermolecular interactions between both ions and CO_2 molecules.[8,21] Reactions of CO_2 with water could lead to carbonic acid and its dissociation products, which leads to a lowering of the IL pH.[29] However, we have considered that the level of the carbonic formation should be small, and thus this effect would not have an important effect on the system features.[17]As concerns to water effect on SO_2 capture, water effect has been only studied for ILs with amine groups. In this case, water molecules would not react with sulfur dioxide molecules.[30] Therefore, the reaction between XO_2 (X = C or S) and water molecules was not considered in this work. Two different approximations, beyond simulations of molecule pairs in gas phase, have been applied. First, the interactions between XO_2 molecules with both ions and the IL have been studied in presence and absence of water molecules. Optimization from those systems composed by one single molecule (e.g., isolated ions) up to systems with four molecules ([CH][LAC] + H_2O + XO_2) were optimized in gas phase (see Figures 1−3). Optimized minima were checked through their vibrational frequencies. For those simulations where two or more molecules are present, different starting points were employed in order to study different starting geometries, focusing our attention on the disposition of minimal energy. All these calculations were carried out using the B3LYP functional,[31] with the 6-31+G** basis sets. Furthermore, dispersion corrections according Grimme's[32] scheme have been also considered along B3LYP functional (B3LYP-D2). Calculated energies after dispersion corrections are comparable with more reliable values, such as those obtained at MP2 level.[33] The Gaussian 09 (revision D.01) package[34] was used for all these calculations.

Second, model clusters with general formula 4YZ, containing four IL pairs plus Y acid gas molecules (Y = 0−3) plus Z water molecules (Z = 0−3), have been optimized in order to get an approach of the fluid properties as a function of the water content as per the studies by Dong et al. showed that intermolecular interactions (mainly H-bonds) between cation and anion are one of the major contribution to ILs features and the study of small ion cluster could describe the structures of the bulk ILs.[28] This approach allows carrying out systematic DFT studies at reasonable computational costs and modeling the bulk properties of the studied systems from a molecular viewpoint, which could allow us to infer the molecular features controlling acid gases capture and the water effect. Clusters with general formula 4YZ were optimized using SIESTA method, which allows optimization with a reduced computational cost for large systems.[35] Optimizations were performed within the Generalized-Gradient approximation (GGA), and the Perdew−Burke−Ernzerhof (PBE) functional,[36] along norm-conserving Troullier−Marting pseudopotentials and numerical double-ζ polarized (DZP) basis set. All atomic positions were relaxed with an energy mesh cutoff of 400 Ry and using the conjugated gradient method, with a force tolerance of 0.04 eV/Å. Aimed at obtaining a reliable geometry for each cluster different starting geometries were assessed. For instance, water and/or gas molecules were randomly added

DOI: 10.1021/acs.jpcb.5b00184
J. Phys. Chem. B 2015, 119, 5546−5557

and/or deleted from a previously optimize clusters of composition 4(Y − 1)Z/4Y(Z − 1). For cluster 400, several structures with each of one having a different relative positions between ions were taken from the central region of previously published molecular dynamic simulations and optimized as previously described.[8] Finally, for each cluster 4YZ, we have picked those optimized geometry with the lowest energy. Grimme's dispersion corrections were also considered;[32] nevertheless, this approach was discarded because very short intermolecular distances were obtained. Finally, single point calculations were carried out over PBE/DZP optimized cluster geometries at the B3LYP/6-31+G** level.

From a molecular point of view, acid gas capture is related with the interaction strength. In this sense, interaction binging energies can be used as a measure of the interaction strength. Binding energies (BE) were calculated as the energy differences among the clusters energy and the sum of corresponding monomer energies at the same level. In addition, binding energies derived from optimizations in gas phase were corrected through counterpoise method to avoid basis set superposition error.[37] In addition to the binging energies, the enthalpies (H) were also estimated at 298.15 K isotherm and 1 atm of pressure. Intermolecular interactions were localized and featured by means of Atoms in Molecules (AIM) theory.[38] Topological analysis according AIM theory was done by using the MultiWFN package.[39] According to Bader's theory,[38] there are four kinds of critical points. Aimed at clarifying the results, we have only focused on those bond critical points (BCP) that rises the criteria for considering the presence of an intermolecular bond. Finally, atomic charges were computed to fit the electrostatic potential according to the ChelpG scheme.[40]

3. RESULTS AND DISCUSSION

3.1. Water Effect on CO_2/SO_2 Capture: Gas-Phase Simulations. Figures 1−3 show the optimized structures (at the B3LYP/6-31+G** level) of the interacting systems considered in this study. Tables 1−7 gather their binding energies (BE), main structural parameters, AIM results, and atomic charges. Although B3LYP and B3LYP-D2 functionals were employed, most of the discussed results refer to the B3LYP functional. All information derived from B3LYP-D2 functional can be found in the Supporting Information (Tables 1S−8S). Though there are some differences, similar results were obtained by using the B3LYP-D2 functional. For instance, B3LYP-D2 tends to provide smaller intermolecular distances, which leads to strengthened interactions.

Table 1. Computed Binding Energies (in Absolute Value, |BE|) for the Studied Systems at B3LYP/6-31+G[a]**

	BE	BE^{BSSE}
I	99.35	97.07
II	3.76	3.39
III	7.23	6.59
IV	11.94	10.89
V	7.59	7.21
VI	22.28	21.04
VII	17.77	16.98
VIII	2.66	2.22
IX	2.23	1.90
X	14.59	13.22
XI	19.05	17.06
XII	15.84	14.10
XIII	28.35	25.84
XIV	102.58	72.94
XV	109.71	64.58
XVI	109.92	92.52
XVII	110.91	108.15
XVIII	116.14	76.20

[a]Units are in kcal mol^{-1}.

3.1.1. Interacting Dimers: [CH][LAC], [ion]-CO_2/SO_2 and [ion]-H_2O. As concerns [CH][LAC] IL, we have focused on the geometry with the largest binding energy. As seen in Figure 1, structure (I), its optimized geometry (using the B3LYP functional), yields several intermolecular bonds labeled as d_1−d_4. Among them, the intermolecular hydrogen bond between the hydroxyl group of [CH] and COO^- [LAC] (d_1) is the strongest one (see Table 3), with a distance equal to 1.602 Å while its electronic density (ρ) is 0.058 au. [CH][LAC] yields a binding energy value (see Table 1) |BE| = 99.35 kcal mol^{-1} at B3LYP/6-31+G**. All these parameters agree with those previously reported for choline benzoate ([CH][BE]) and choline salicylate ([CH][SA]) ILs at B3LYP/6-311+G**.[41] As discussed below, both levels provide comparable values. In this sense, it is known that the selected basis set has no important effects on interaction energies since the major contribution is due to the charge−charge attraction.[42] When empirical dispersion corrections are considered (B3LYP-D2/6-31+G**), only slight differences are obtained for [CH][LAC] optimized geometry (see Table 3S and Figure 1S). As expected, whether dispersion corrections are considered, the main interaction (d_1) is established between OH^- (choline) and COO^- (lactate) groups. Intermolecular bond d_2 and d_3 distances suffer a slender shortening of 0.217 and 0.104 Å, respectively, while d_3 is elongated due to the inclusion of the dispersion term in the applied functional. The binding energy calculated at the B3LYP-D2/6-31+G** level (|BE| = 129.35 kcal mol^{-1}) is larger than the value obtained without dispersion corrections. Counterpoise correction provides energies with less approximately 2% of the uncorrected energy. Prior to the analysis of the interactions between [CH][LAC] and CO_2/SO_2 and water effect, interactions between isolated ions and water and/or CO_2/SO_2molecules were studied. Optimized structures of [CH]-CO_2/SO_2 and [CH]-H_2O pairs are showed in Figure 1 (structures II, III, IV). CO_2/SO_2 or H_2O molecules set up and hydrogen bond with choline cation (labeled as d_5/d_6 and d_8, respectively, where the H atom of hydroxyl group (of choline cation) plays a hydrogen bond donor in the intermocular H-bond between choline and CO_2/SO_2 or H_2O molecules). [CH]-SO_2 (III) also presents an additional intermolecular interaction (d_7) between the O atom of SO_2 and H of $-CH_2$ adjacent to hydroxyl group (at B3LYP-D2, this intermolecular interaction is found between O atoms in SO_2 and H of to $-CH_2$ adjacent to N; see Figure 1S). However, the electronic density of d_7 is smaller than the value obtained for d_6, mainly due to a larger intermolecular distance; thus, small contribution to the binding energy is expected from this interaction. As seen in Tables 1, 3, and 6, there is clear relationship between binding energies, intermolecular distances, and their electronic densities of the corresponding BCPs. Thus, $d_8 < d_6 < d_5$, while |BE| follows the same pattern: H_2O (11.94 kcal mol^{-1}) > SO_2 (7.23 kcal mol^{-1}) > CO_2 (3.76 kcal mol^{-1}).

[LAC] anion interacts with CO_2/SO_2 or water molecule through its COO^- group in a T-shaped way (see structures V−

DOI: 10.1021/acs.jpcb.5b00184
J. Phys. Chem. B 2015, 119, 5546−5557

Table 2. Released Energies (in Absolute Value, $|\Delta E|$) of Different Processes Related to Acid Gas Capture by [CH][LAC] (eqs 1a/b−8a/b) at B3LYP/6-31+G[a]**

		(a) CO_2	(b) SO_2
1	$[CH]-XO_2 + H_2O \rightarrow H_2O-[CH]-XO_2$	10.83	11.82
2	$[CH]-H_2O + XO_2 \rightarrow H_2O-[CH]-XO_2$	2.65	7.11
3	$[LAC]-XO_2 + H_2O \rightarrow H_2O-[LAC]-XO_2$	8.25	6.06
4	$[LAC]-H_2O + XO_2 \rightarrow H_2O-[LAC]-XO_2$[b]	−1.94	10.57
5	$[CH][LAC] + XO_2 \rightarrow [CH][LAC]-XO_2$	3.23	10.37
6	$[CH][LAC] + H_2O \rightarrow [CH][LAC]-H_2O$	10.57	10.57
7	$[CH][LAC]-H_2O + XO_2 \rightarrow H_2O-[CH][LAC]-XO_2$	0.99	6.23
8	$[CH][LAC]-XO_2 + H_2O \rightarrow H_2O-[CH][LAC]-XO_2$	8.33	6.43
9	$[CH][LAC] + XO_2 + H_2O \rightarrow H_2O-[CH][LAC]-XO_2$	11.56	16.79

[a]Units are in kcal mol^{-1}. [b]Negative values means that for such process it would be necessary to provide energy.

Table 3. Main Structural Parameters of Optimized Dimers I−IX at B3LYP/6-31+G[a]**

		gas phase		
		B3LYP/6-31+G**		
I	d_0	1.946	d_1	1.602
	α_1	104.3	d_2	2.526
	τ_1	1.1	d_3	2.044
	α_2	107.7	d_4	2.184
	τ_2	132.7		
II	α_2	110.2	α_3	179.7
	τ_2	180.0	d_5	2.030
III	α_2	109.7	d_6	2.011
	τ_2	164.5	d_7	2.846
	α_4	116.6		
IV	α_2	110.0	α_5	106.1
	τ_2	−180.0	d_8	1.785
V	d_0	1.844	α_3	168.8
	α_1	100.9	d_9	2.984
	τ_1	0.8	d_{10}	2.559
VI	d_0	1.917	α_4	114.5
	α_1	103.7	d_{11}	2.235
	τ_1	0.5		
VII	d_0	1.853	α_5	97.4
	α_1	101.3	d_{12}	1.978
	τ_1	0.6	d_{13}	2.099
VIII	α_3	177.8	d_{14}	2.837
	α_5	106.3		
IX	α_4	117.9	d_{15}	2.791
	α_5	105.7		

[a]Distances (d) are in Å; angles (α) and dihedral angles (τ) are in degrees. See Figure 1 for labeling. d_0, α_{1-5}, and τ_{1-2} are intermolecular parameters for [CH], [LAC], CO_2, SO_2, and H_2O molecules.

Table 4. Main Structural Parameters for Optimized Trimers X-XVI at B3LYP/6-31+G[a]**

		gas phase		
		B3LYP/6-31+G**		
X	α_2	109.1	d_{16}	2.564
	τ_2	179.2	d_{17}	2.887
	α_3	178.2	d_{18}	1.727
	α_5	105.2	d_{19}	2.313
XI	α_2	108.4	d_{20}	2.499
	τ_2	167.2	d_{21}	3.663
	α_4	117.5	d_{22}	1.778
	α_5	107.2	d_{23}	2.178
XII	d_0	2.506	d_{24}	2.904
	α_1	108.3	d_{25}	1.636
	τ_1	52.5	d_{26}	2.003
	α_3	173.6	d_{27}	2.482
	α_5	103.3		
XIII	d_0	1.604	d_{28}	2.472
	α_1	97.5	d_{29}	2.307
	τ_1	−2.8	d_{30}	1.931
	α_4	115.8	d_{31}	2.200
	α_5	103.5		
XIV	d_0	1.921	d_{32}	1.590
	α_1	103.8	d_{33}	2.586
	τ_1	1.1	d_{34}	2.188
	α_2	107.8	d_{35}	2.065
	τ_2	−133.1	d_{36}	2.718
	α_3	175.9		
XV	d_0	1.787	d_{39}	1.651
	α_1	101.2	d_{40}	2.172
	τ_1	8.2	d_{41}	2.164
	α_2	107.4	d_{42}	2.447
	τ_2	−137.3	d_{43}	2.456
	α_4	116.0	d_{44}	2.745
XVI	d_0	1.956	d_{46}	1.703
	α_1	104.4	d_{47}	3.145
	τ_1	−0.7	d_{48}	2.642
	α_2	106.8	d_{49}	1.720
	τ_2	−105.2	d_{50}	2.425
	α_5	105.7		

[a]Distances (d) are in Å; angles (α) and dihedral angles (τ) are in degrees. See Figure 2 for labeling. d_0, α_{1-5}, and τ_{1-2} are intermolecular parameters for [CH], [LAC], CO_2, SO_2, and H_2O molecules.

VII in Figure 1). CO_2 yields two intermolecular interactions with COO^-, with d_{10} being more geometrically favored. Intermolecular distance d_{10} between COO^- and CO_2 is 0.32 Å larger than the intermolecular bond between [LAC] and SO_2 molecule (d_{11}), which also yields a larger electronic density value. Moreover, there is an important charge transfer (Table 7) between [LAC] and SO_2 molecule. Both factors (shorter intermolecular bonds and charge transfer process) agree with higher binding energy of [LAC]−SO_2 system. Both H atoms of water molecule establish interactions with both O of COO^- groups with distances of approximately 2.0 Å. Although intermolecular distances between [LAC] and water molecule are shorter than [LAC]−SO_2 ones, the higher charge transfer from [LAC] anion up to SO_2 molecule (see Table7) could explain the major anion preference with regard to the SO_2 molecule. As seen, both ions prefer interaction with water molecules instead of CO_2, while [LAC] anion shows greater

DOI: 10.1021/acs.jpcb.5b00184
J. Phys. Chem. B 2015, 119, 5546−5557

Table 5. Main Structural Parameters for Optimized Tetramers XVII and XVIII at B3LYP/6-31+G**[a]

		gas phase		
		B3LYP/6-31+G**		
XVII	d_0	2.602	d_{52}	2.394
	α_1	109.4	d_{53}	2.207
	τ_1	59.1	d_{54}	2.021
	α_2	107.9	d_{55}	2.795
	τ_2	−111.3	d_{56}	3.027
	α_3	175.9	d_{57}	1.717
	α_5	105.1	d_{58}	2.055
	d_{51}	1.668	d_{59}	2.552
XVIII	d_0	2.575	d_{62}	2.408
	α_1	110.1	d_{63}	2.220
	τ_1	56.1	d_{64}	2.028
	α_2	108.1	d_{65}	2.562
	τ_2	−111.3	d_{66}	2.938
	α_4	116.5	d_{67}	1.749
	α_5	104.8	d_{68}	1.890
	d_{61}	1.681	d_{70}	2.284

[a]Distances (d) are in Å; angles (α) and dihedral angles (τ) are in degrees. See Figure 3 for labeling. d_0, $\alpha_{1\text{-}5}$, and $\tau_{1\text{-}2}$ are intermolecular parameters for [CH], [LAC], CO_2, SO_2, and H_2O molecules.

preference for sulfur dioxide (Table 1). For either CO_2/SO_2 or water, binding energies of [LAC] anion are larger than those of [CH] cation. As expected, binding energies between both ions are larger (mainly due to electrostatic interactions) than those between ion and CO_2/SO_2 or H_2O. XO_2 or H_2O molecules interact with [CH]/[LAC] ions through hydroxyl/COO^- groups. The interaction between both ions is also located through the same functional groups. Therefore, OH/COO^- groups could be labeled as *active sites* in the corresponding [CH]/[LAC] ions.

Reported results for ion−CO_2 interactions are in agreement with those previously reported at B3LYP/6-311+G**. For example, we previously reported 7.12 kcal mol^{-1} (in absolute value) for [LAC]-CO_2 interaction computed at B3LYP/6-311+G**, which is very similar to the value reported in this work (7.59 kcal mol^{-1}), computed at B3LYP/6-31+G**.

3.1.2. Interacting Trimers: H_2O−[ion]−CO_2/SO_2. As seen, when only water or XO_2 molecules are present, all of them interact with [CH]/[LAC] ions through their *active sites*. Therefore, the preference of both isolated ions with regard to water and XO_2molecules was analyzed considering systems composed by one ion ([CH] or [LAC]), one XO_2 molecule and one water molecule (see structures X-XIII in Figure 2). Besides, several process (eqs 1a/b−4a/b) related with CO_2/SO_2 (labeled as a/b, respectively) adsorption in water presence have been defined and released energy (ΔE) calculated (see Table 2 and Table 2S):

$$[CH]{-}CO_2/SO_2 + H_2O \rightarrow H_2O{-}[CH]{-}CO_2/SO_2 \quad (1a/b)$$

$$[CH]{-}H_2O + CO_2/SO_2 \rightarrow H_2O{-}[CH]{-}CO_2/SO_2 \quad (2a/b)$$

$$[LAC]{-}CO_2/SO_2 + H_2O \rightarrow H_2O{-}[LAC]{-}CO_2/SO_2 \quad (3a/b)$$

$$[LAC]{-}H_2O + CO_2/SO_2 \rightarrow H_2O{-}[LAC]{-}CO_2/SO_2 \quad (4a/b)$$

Table 6. Electronic Density (ρ) and Its Laplacian ($\nabla^2\rho$) for Intermolecular Interactions at B3LYP/6-31+G**[a]

		gas phase			
		B3LYP/6-31+G**			
		ρ	$\nabla^2\rho$	ρ	$\nabla^2\rho$
I	d_0	0.030	0.098	d_3 0.021	0.068
	d_1	0.058	0.148	d_4 0.030	0.098
	d_2	0.010	0.033		
II	d_5	0.017	0.058		
III	d_6	0.020	0.060	d_7 0.005	0.017
IV	d_8	0.035	0.107		
V	d_0	0.037	0.111	d_{10} 0.020	0.062
VI	d_0	0.031	0.101	d_{11} 0.061	0.141
VII	d_0	0.036	0.110	d_{13} 0.026	0.068
	d_{12}	0.020	0.056		
VIII	d_{14}	0.010	0.041		
IX	d_{15}	0.006	0.022		
X	d_{16}	0.007	0.028	d_{18} 0.045	0.134
	d_{17}	0.010	0.039	d_{19} 0.011	0.043
XI	d_{20}	0.004	0.015	d_{23} 0.013	0.048
	d_{22}	0.036	0.110		
XII	d_{24}	0.010	0.037	d_{26} 0.024	0.064
	d_{25}	0.053	0.144	d_{27} 0.008	0.032
XIII	d_0	0.064	0.157	d_{30} 0.025	0.075
	d_{28}	0.011	0.037	d_{31} 0.013	0.042
	d_{29}	0.053	0.130		
XIV	d_0	0.032	0.101	d_{34} 0.018	0.050
	d_{32}	0.060	0.149	d_{35} 0.021	0.065
	d_{33}	0.009	0.030	d_{36} 0.013	0.051
XV	d_0	0.042	0.126	d_{41} 0.040	0.104
	d_{39}	0.051	0.137	d_{42} 0.011	0.036
	d_{40}	0.018	0.052	d_{43} 0.006	0.024
XVI	d_0	0.029	0.097	d_{49} 0.041	0.123
	d_{46}	0.042	0.132	d_{50} 0.011	0.033
	d_{48}	0.018	0.048		
XVII	d_{51}	0.048	0.135	d_{57} 0.043	0.127
	d_{52}	0.013	0.038	d_{58} 0.021	0.060
	d_{54}	0.017	0.046	d_{60} 0.007	0.028
	d_{55}	0.012	0.045		
XVIII	d_{61}	0.047	0.132	d_{65} 0.014	0.083
	d_{62}	0.009	0.030	d_{67} 0.040	0.118
	d_{63}	0.009	0.045	d_{68} 0.030	0.083
	d_{64}	0.012	0.037	d_{69} 0.012	0.043

[a]All values in au.

Equation 1a describes the released energy for the interaction between [CH] and water, when [CH] is previously interacting with CO_2. The released energy of this process has been calculated as the difference between binding energies of structures X and II. As seen in Figure 2, for structures X and XI, water molecules occupy the choline cation active sites. The distance between [CH] and water molecule (d_{18}/d_{22} for CO_2/SO_2) is around 1.76 Å, very close to the intermolecular distance found for [CH]−H_2O couple (d_8 = 1.78 Å). The presence of XO_2 incites a slight strengthening on the interaction between water and hydroxyl group. Since water obstructs the *active site* of choline cation, XO_2 is forced to interact with [CH] cation through intermolecular bonds between side O atoms of CO_2/SO_2 and CH_2 group adjacent to N atom (d_{16}/d_{20}) of C/S atom and O atom of hydroxyl group (d_{17}/d_{21}). There is also an intermolecular hydrogen bond between XO_2 and water molecule (d_{19}/d_{23}). All these intermolecular interactions high

DOI: 10.1021/acs.jpcb.5b00184
J. Phys. Chem. B 2015, 119, 5546−5557

Table 7. Computed Atomic Charges Sums in Gas Phase According to the ChelpG Scheme at B3LYP/6-31+G over the Cation (q^{CH}), the Anion (q^{LAC}), CO_2 (q^{CO_2}), SO_2 (q^{SO_2}), and H_2O (q^{H_2O}) Molecules for Optimized I−XIV Systems**

	gas phase			
	B3LYP/6-31+G**			
	q^{CH}	q^{LAC}	q^{XO_2}	q^{H_2O}
I	0.81	−0.81		
II	0.99		0.01	
III	0.96		0.04	
IV	0.99			0.01
V		−0.90	−0.10	
VI		−0.65	−0.35	
VII		−0.96		−0.04
VIII			0.00	0.00
IX			0.00	0.00
X	0.93		0.02	0.05
XI	1.00		0.08	−0.08
XII		−0.89	−0.07	−0.04
XIII		0.67	−0.24	−0.09
XIV	0.86	−0.82	−0.04	
XV	0.89	−0.72	−0.17	
XVI	0.84	−0.78		−0.05
XVII	0.84	−0.71	−0.04	−0.09
XVIII	0.81	−0.64	−0.08	−0.09

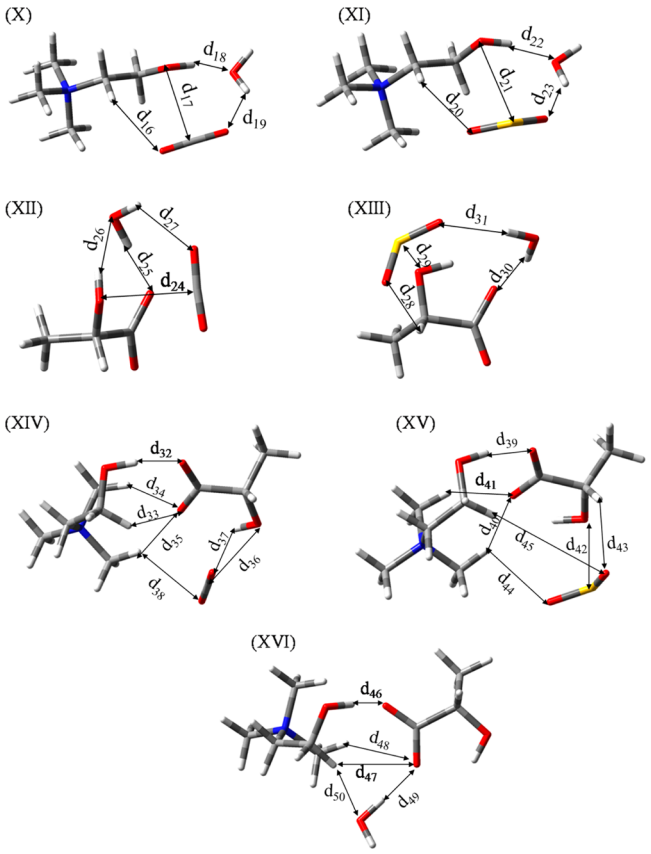

Figure 2. Molecular structure for optimized trimers optimized at B3LYP/6-31+G** level along main optimized structure parameters: (X) CO_2−[CH]−H_2O, (XI) SO_2−[CH]−H_2O, (XII) CO_2−[LAC]−H_2O, (XIII) SO_2−[LAC]−H_2O, (XIF) IL−CO_2, (XV) IL−SO_2, and (XVI) IL−H_2O. Atom color code: (gray) carbon, (red) oxygen, (yellow) sulfur, (blue) nitrogen, and (light gray) hydrogen.

distances and low ρ values, pointing out to a weakening on XO_2 by [CH] upon water presence. Thus, water molecule would be able to move the CO_2/SO_2 molecule from the *active site* of the choline cation. Processes 1a/b yield $|\Delta E|$= 10.83 kcal mol^{-1} and $|\Delta E|$= 11.82 kcal mol^{-1}. Unfortunately, CO_2/SO_2 capture in water presence yields lower released energy (2.65/7.11 kcal mol^{-1}). According to the B3LYP-D2/6-31+g** level, CO_2 capture by [CH] cation in water presence would require energy, instead of releasing it. SO_2 capture is a more favored process even upon water presence.

COO^- group is the [LAC] *active site*, which interacts with CO_2/SO_2 or H_2O molecules. In the presence of both CO_2/SO_2 and H_2O molecules, there is an arrangement that allows the OH group to also interact with CO_2/SO_2. Thus, the hydroxyl group of the lactate anion should be also included in the definition of *active site*. In addition, in the presence of both CO_2 and H_2O, intramolecular bonds between OH and COO^- groups in the [LAC] anion (labeled as d_0) are broken. According to the optimized geometry of H_2O−[LAC]−CO_2 (see structure XII in Figure 2), CO_2 molecule establishes one intermolecular bond between the C (CO_2) and the O atom of the COO^- group (d_{24}), while the water molecule is linked to both OH and COO− groups (d_{25} and d_{26}). Again, there is also an intermolecular bond between water and CO_2 molecules (d_{27}). The presence of both CO_2 and water molecules causes the hydroxyl dihedral angles (labeled as τ_1) to take a value equal to 52.5°. Such a dihedral angle hinders the formation of the intermolecular bond in lactate molecule (defined as d_0 in Figure 1). Interactions between [LAC] and water molecules in CO_2 presence are larger than [LAC]−CO_2 interactions in water presence. In fact, released energy for process 3a is higher than that for process 4a, which yields energy with opposite sign at B3LYP/6-31+G** level. Regarding H_2O−[LAC]−SO_2 (see structure XIII in Figure 2), SO_2 molecule interacts with the OH [LAC] group (S−O, d_{29}). Sulfur dioxide is also bonded to the CH group adjacent to hydroxyl (d_{28}); however, this bond yields small ρ (0.0011 au), pointing out that the main link between [LAC] and SO_2 molecule is d_{29}. The water molecule yields intermolecular interactions with the SO_2 (d_{31}) and COO^- group (d_{30}). Electronic density value of d_{29} is larger than those of d_{30} and d_{31} (see Table 6), which suggests greater anion preference for SO_2 molecules. In fact, capture of SO_2 in the presence of water by [LAC] anion (eq 4b) is more favorable than capture of H_2O in the presence of SO_2 (eq 4a/ba). Note that SO_2 does not lead to breakage of d_0 intermolecular interaction in [LAC]. Even in the presence of water, [LAC] anion transfers negative charge up to up to SO_2 molecule. In brief, the [LAC] *active site* is not preferentially occupied by one molecule, but there is an arrangement in which both water and XO_2 molecules can interact with [LAC] anion. Water obstructs XO_2 capture, with the effects being greater for CO_2. Even in the presence of water, [LAC] anion would be more efficient than [CH] cation for XO_2 capture.

3.1.3. Interacting Trimers: [CH][LAC]-CO_2/SO_2 and [CH]-[LAC]-H_2O. Figure 2 (structures XIV/XV and XVI) displays the optimized geometries of [CH][LAC]−XO_2 and [CH][LAC]−H_2O. Released energies for acid gas capture using choline lacate IL as well as water−IL interactions are described as follows:

$$[CH][LAC] + CO_2/SO_2 \rightarrow [CH][LAC]{-}CO_2/SO_2 \quad (5a/b)$$

$$[CH][LAC] + H_2O \rightarrow [CH][LAC]{-}H_2O \quad (6)$$

DOI: 10.1021/acs.jpcb.5b00184
J. Phys. Chem. B 2015, 119, 5546−5557

Previous theoretical simulations on [CH][LAC] IL shown that the molecular-level structuring of IL is not affected by the presence of CO_2 or water molecules.[8,21] Our DFT simulations show that the presence of CO_2/SO_2 or water does not induce important changes on the relative interaction between ions. As seen for isolated [CH][LAC], the main interaction between [CH] and [LAC] ions is established through their active sites, i.e., the hydroxyl of [CH] cation is directed toward the COO^- of [LAC] anion (d_{32}/d_{39} and d_{46} for CO_2/SO_2 and H_2O, respectively). As seen in Table 3, these hydrogen bonds between ions yield d_{32} = 1.590 Å/d_{39} = 1.651 Å and d_{46} = 1.703 Å and ρ = 0.060/0.051 au and ρ = 0.042 au for CO_2/SO_2 and water molecules, respectively. The presence of water molecule is able to provide the largest separation between both ions, which means a weakening of the interaction between ions. As seen above for XO_2−cation/anion and H_2O−cation/anion systems (structures II−VII), the lactate anion provided the largest binding energies, where the main interaction between CO_2/SO_2 or H_2O molecules was established through the *active site* of lactate anion (COO^-). Nonetheless, for the IL, the *active site* of lactate anion (COO^-) is occupied by the cation. Thus, the CO_2/SO_2 molecule is forced to interact with [LAC] anion through hydroxyl group. Then, OH group of [LAC] anion should be also included in the definition of active site of lactate anion. CO_2 is linked to [LAC] group through an intermolecular bond (d_{36}) between C (CO_2) and O (hydroxyl), with d =2.718 Å and ρ = 0.013 au. The optimized structure at the B3LYP-D2/6-31+G** level also yielded a hydrogen bond (d_{37} = 2.740 Å, ρ = 0.010 au) between O (CO_2) and H (hydroxyl group). SO_2 molecule is able to set up two intermolecular bonds with [LAC] anion (d_{42} and d_{43}). The first is similar than d_{36}, that is, between S atom (SO_2) and O (hydroxyl), with d = 2.447 Å and ρ = 0.011 au

CO_2/SO_2 molecule does not cause the break of d_0 intermolecular bond of [LAC] anion, which is slightly strengthened upon the presence of SO_2 molecule (larger ρ value than for isolated IL and for the CO_2 or H_2O presence).

As previously mentioned, the presence of hydroxyl groups would provide strong interactions between the cation and the gas molecule.[25,26] However, OH group of choline is fully occupied by [LAC] anion and thus CO_2 is forced to interact with terminal methyl group (d_{38}), while SO_2 does with both methyl (d_{44}, only at B3LYP-D2 level) and CH_2 (d_{45}, only at B3LYP-D2 level). These interactions between [CH] cation and CO_2/SO_2 molecule are weaker than those interactions found for structures II−IV. Regarding to water molecule, the main interaction is and hydrogen bond (d_{49} = 1.720 Å and ρ = 0.041 au) with COO^- of lactate anion. The smaller size of water molecule allows an approach toward [LAC] anion, which enables shorter intermolecular distances and larger electronic density values than XO_2. Water molecule also presents a weak hydrogen bond choline through CH_2 group adjacent to OH (d_{50}). Based on structural and electron density parameters, it is clear that [CH][LAC] stronger interacts with water molecule. Nevertheless, $|\Delta E|$ = 3.23 kcal mol^{-1} for CO_2 capture by [CH][LAC] (eq 5a/b), while this value increases up to $\simeq$ 10.5 kcal mol^{-1} for SO_2 and H_2O capture; that is, [CH][LAC] yields similar preference to interact with SO_2 or water molecules. As previously noted, there is also a charge transfer from [LAC] anion up to SO_2 molecule, which could explain the high released energy for SO_2 capture despite weaker interactions in comparison with water.

3.1.4. Interacting Tetramers: H_2O-[CH][LAC]-CO_2/SO_2. Figure 3 draws optimized structures of H_2O−[CH][LAC]−CO_2/SO_2 tetramers. Structures XVII and XVIII show some structural similarities in comparison with structure XVI (IL−H_2O). The main intermolecular bond between ions (d_{51}/d_{61} for CO_2/SO_2 capture) is found between OH of choline and COO^- of lactate, whose distance (d_{51} = 1.668 Å/d_{61} = 1.681 Å) is slightly shorter than the cation−anion intermolecular bond of [CH][LAC]−H_2O (d_{46} = 1.703 Å). Similar trend is found for the corresponding electronic density values. As seen for [CH][LAC]−H_2O, water molecule mainly forms a hydrogen bond with COO^- group of lactate, with d_{57} = 1.717 Å/d_{67} = 1.749 Å and ρ = 0.043 au/0.040 au. The hydrogen bond between water molecule and COO^- of lactate (d_{57}/d_{67}) displays similar features than those previously found for structure XVI (d_{49}). In addition, O atom of water molecule also interacts with OH group of lactate ((d_{58} = 2.055 Å/d_{68} = 1.890 Å, ρ = 0.021 au/0.030 au). Note that one H of water interacts with XO_2 (d_{60}/d_{70}). This interaction between water and XO_2 molecule brings out and approaches between water and OH of lactate anion ease this new hydrogen bond. Short distances and higher electronic density of d_{68} respecting d_{58} points out that the interaction between water molecule and OH group of [LAC] anion is scarcely strengthened upon XO_2 presence. CO_2/SO_2 also presents an intermolecular bond with hydroxyl of [LAC] anion (d_{55} = 2.795 Å/d_{65} = 2.562 Å and ρ = 0.012 au and 0.014 au). Note that the hydroxyl group of the [LAC] anion is involved in the interactions with both XO_2 and H_2O molecules. Thereby, d_0 intramolecular hydrogen bond is broken allowing H acts as acceptor of d_{58}/d_{68} intermolecular bonds. The processes related with XO_2 capture in the presence of water and *viceversa* as well as the capture of both molecules by [CH][LAC] IL have been described as

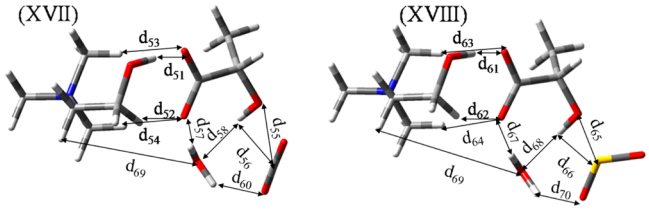

Figure 3. Molecular structure for optimized tetramers optimized at the B3LYP/6-31+G** level along main optimized structure parameters: (XVII) CO_2−IL−H_2O and (XVIII) SO_2−IL−H_2O. Atom color code: (gray) carbon, (red) oxygen, (yellow) sulfur, (blue) nitrogen, and (light gray) hydrogen.

$$[CH][LAC]{-}H_2O + CO_2/SO_2 \rightarrow H_2O{-}[CH][LAC]{-}CO_2/SO_2 \quad (7a/b)$$

$$[CH][LAC]{-}CO_2/SO_2 + H_2O \rightarrow H_2O{-}[CH][LAC]{-}CO_2/SO_2 \quad (8a/b)$$

$$[CH][LAC] + H_2O + CO_2/SO_2 \rightarrow H_2O{-}[CH][LAC]{-}CO_2/SO_2 \quad (9a/b)$$

CO_2 capture in the presence of water (eq 7a) is not be highly favored (ΔE = 0.99 kcal mol^{-1}), while the same value is much higher for SO_2 capture ($|\Delta E|$ =6.23 kcal mol^{-1}). Both values are smaller than those obtained in absence of water (eq 5a/b); that

DOI: 10.1021/acs.jpcb.5b00184
J. Phys. Chem. B 2015, 119, 5546−5557

Table 8. Thermodynamic Parameters (ΔH) of Processes Defined in Eqs 5−9 Estimated at the B3LYP/6-31+G** Level[a]

		ΔH	
		(a) CO_2	(b) SO_2
5	$[CH][LAC] + XO_2 \rightarrow [CH][LAC]{-}XO_2$	−2.30	−9.00
6	$[CH][LAC] + H_2O \rightarrow [CH][LAC]{-}H_2O$	−8.50	
7	$[CH][LAC]{-}H_2O + XO_2 \rightarrow H_2O{-}[CH][LAC]{-}XO_2$	−1.72	−4.61
8	$[CH][LAC]{-}XO_2 + H_2O \rightarrow H_2O{-}[CH][LAC]{-}XO_2$	−4.08	−4.12
9	$[CH][LAC] + XO_2 + H_2O \rightarrow H_2O{-}[CH][LAC]{-}XO_2$	−8.64	−13.11

[a]Units are in kcal mol^{-1}.

is, water presence decreases released energy for XO_2 capture. Though water presence has important drawbacks on ΔE for CO_2/SO_2 capture, the water molecule is able to interact with the IL even in the presence of XO_2 molecule. However, the larger value of eq 8a indicates that the CO_2 molecule is more easily displaced by water presence. In short, the water molecule tends to block the *active site* of choline benzonate, which hinders CO_2/SO_2 capture, with CO_2 being more affected by water presence. Note that eq 7a and b yields similar ΔE values for SO_2 capture in the presence of water and vice versa. Then, it could be a competition between both molecules to interact with [CH][BE], in which *active sites* are preferably occupied by water. According with eq 9a/b, [CH][BE] should be able to capture both molecules. Most of this released energy ($|\Delta E|$ = 11.56 kcal mol^{-1}/16.79 kcal mol^{-1}) comes from IL−water interactions. Furthermore, this process can be described as a sequential process: first IL catches one water molecule (eq 6); then, this trimer could cop the XO_2 molecule (eq 7a/b). In fact, the sum of released energies of eqs 6 and 8a/b is equal to the released energy of eq 9a/b.

An estimation of thermodynamic properties helps in understanding the energetics associated with acid gas capture by ILs by [CH][LAC] and water effects as well (eqs 5−9) (Table 8). All these processes give $\Delta H < 0$; that is., there is a release of heat. Both released energies (ΔE) and ΔH follow the same trend. ΔG and ΔS are also lower than zero, which agrees with spontaneous processes. ΔG also follows a similar pattern as ΔE, while ΔS lies between 0.00 and −0.07 kcal/mol. Therefore, we have focused on the enthalpy values as a measurement of the released heat of those processes described by eqs 5−9. In general terms, the tendency of ΔH is similar to that of ΔE, showing how CO_2 capture by [CH][LAC] is less favored than SO_2 capture in concordance with less negative ΔH released energy and lower ΔE of eqs 5a, 7a, and 8a. Water presence has important drawbacks on the enthalpy values. As previously noted from released energy values, these [CH]-[LAC]$-CO_2$ interactions are more affected by water molecule.

3.2. Cluster Approximation. In the previous sections, water effect on XO_2 capture has been assessed through systems formed by one molecule of IL, one XO_2, and one H_2O. At the macroscopical level, the water effect on XO_2 capture is directly related with XO_2 and H_2O solubility in the bulk. Dong et al. proved that the study of small ion clusters could describe the main structural features of the bulk configuration in ILs.[28] Then this section mainly pursues obtaining information about the water effect on CO_2/SO_2 by [CH][LAC] through the study of small clusters. Properties such as binding energies, intermolecular interactions, and atomic charges (Figures 4−6 and Tables 9S, 10S) have been analyzed for small clusters with composition 4YZ, that is, 4 ionic pairs, Y/Z molecules of water/XO_2 (Y/Z = 0−3). All these properties have been assessed for each cluster as a whole. Table 9S gathers computed binding

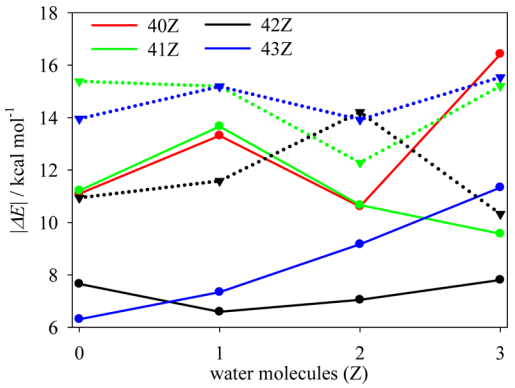

Figure 4. Released energies (in absolute value, $|\Delta E|$) for 4YZ clusters as a function of the water molecules (Z) for CO_2/SO_2 adsorption (solid/dotted lines).

energies at B3LYP/6-31+G** level. The values corresponding to isolated units were obtained from previous sections. Cluster 400 yields |BE| = 99.32 kcal mol^{-1} per ionic pair, which is very close to that computed for the isolated [CH][LAC] ionic pair (99.35 kcal mol^{-1}). This suggests that the main driving force in the IL bulk would be the intermolecular interactions and coulomb attraction between both ions as described for structure I. This shows a prevailing role of short-range interaction on the fluid structure. Table 9S also collects released energies calculated as the difference energies computed for each cluster and the binding energy for the isolated [CH][LAC] ionic pair (4 times). For cluster 400, this released energy would be related with other intermolecular interactions not described through structure I. Figure 4 plots the evolution of $|\Delta E|$ as water quantity (Z) function. In the absence of XO_2 molecules (40Z), $|\Delta E|$ tends to increase with the number of water molecules. In general, energies of 400 cluster and clusters with SO_2 lie between 11.0 kcal mol^{-1} and 16.0 kcal mol^{-1}, close to the range reported for eqs 5−9 in Table 2. In agreement with reported results from gas phase calculations, $|\Delta E|$ for SO_2 capture is less affected by water molecules. Furthermore, the similarity of the released energies for SO_2 and water capture (even in the presence of other molecules) can be related with a equilibrium between SO_2 or water molecules occupying *active site* of the IL, slight favored toward water molecules.

The main results from AIM analysis are shown in Table 10S and Figure 5. The total number of bond critical points (n) increases with the number of molecules in the cluster. Table 10S and Figure 5 also exhibit the total sum of electronic density for all BCPs (ρ) and the average value for each BCP (ρ/n). As expected, the total ρ increases with n. Those clusters with the same number of water and XO_2 molecules provide usually higher values for SO_2, which agrees with an improved SO_2 capture by [CH][LAC]. Cluster with SO_2 provided larger m

DOI: 10.1021/acs.jpcb.5b00184
J. Phys. Chem. B 2015, 119, 5546−5557

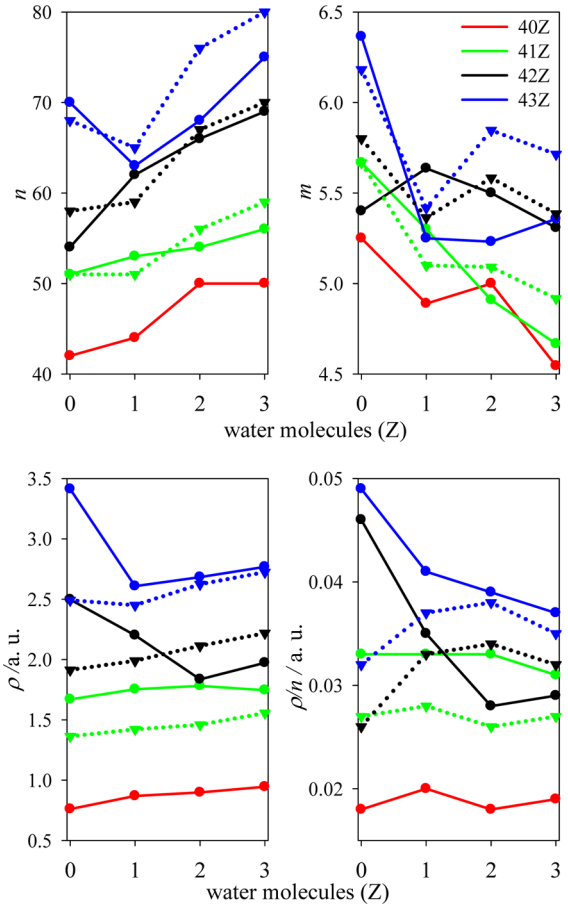

Figure 5. Total number of BCP (n), number of BPC per molecule ($m = n/(4 \times 2 + Y + Z)$), total sum of their electronic density values (ρ), and the average value per BCP (ρ/n) for intermolecular interactions obtained for 4YZ clusters. Solid/dotted lines correspond to CO_2/SO_2 adsorption.

values (m has been estimated as average number of interactions per molecule) than for clusters CO_2. However, m decreases upon water quantity. Water molecules fill the space between ions, which hinder their interactions and interactions between IL and XO_2 as well. The average electronic density value per BCP also decreases with the water quantity. It is clear than water presence has important drawback on XO_2 capture by [CH][LAC]. As previously shown in Table 7 for structures XIV−XVIII, [CH] cation presents a positive charge ~0.85 e^-, similar than those ones computed for [CH][LAC] pair. However, lactate becomes less negative in the presence of other molecules. [LAC] charge decreases from 0.81 e^- (structure I) up to 0.78 e^-, 0.71 e^-, and 0.64 e^- for structures XVI, XVII, and XVIII. The largest changes are due to the sulfur dioxide molecule. Figure 6 and Table 11S collect charge evolution of both ions, XO_2 and water molecules. Charge over choline cation (q^{CH}, red line) lies between 0.83 e^-/0.80 e^- and 0.78e^-/0.74 e^- in the presence of CO_2/SO_2 molecule, while q^{CH} = 0.78e^- (average value per cation) for cluster 400. Clusters 433 provided the largest differences over q^{CH} regarding cluster 400. However, these changes are 0.05 and 0.04 for CO_2/SO_2 in comparison with cluster 400. Negative charge over lactate anion (q^{LAC}, green line in Figure 6) is equal to 0.78 e^- for cluster 400. However, lactate becomes less negative in the presence of XO_2 and water molecules. As seen above, there is a charge transfer from the lactate up to SO_2. Thus, SO_2 molecules bring out the largest changes over q^{LAC}. For both clusters 433, negative charge over lactate is around 0.66 e^-. The same value for both CO_2 and SO_2 could indicate that, in the presence of water, [LAC] anion mainly interacts with water molecules instead of CO_2/SO_2. XO_2 and water charges (q^{XO_2} and q^{H_2O}, blue and black lines, respectively) are collected as the total charge over all XO_2 or water molecules. q^{XO_2} tends to be zero with increasing water presence. In addition, q^{XO_2} is more affected by water than q^{H_2O} in the presence of XO_2. Both facts also point out that [CH][LAC] interacts stronger with water molecules.

4. CONCLUSIONS

This study investigates the suitability of [CH][LAC] IL as CO_2/SO_2 capture agent as well as the effect of water on the acid-gas capture process through DFT simulations. Being a pioneer study that investigates the possibility of the application of [CH][LAC] for SO_2 absorption, computational methods have allowed gaining further insight up to the interaction mechanism at the molecular level. Two different approximations have been applied: (i) gas phase simulations on model systems considering up to four molecules ([CH], [LAC], H_2O and CO_2/SO_2) and (ii) more realistic approximation to the

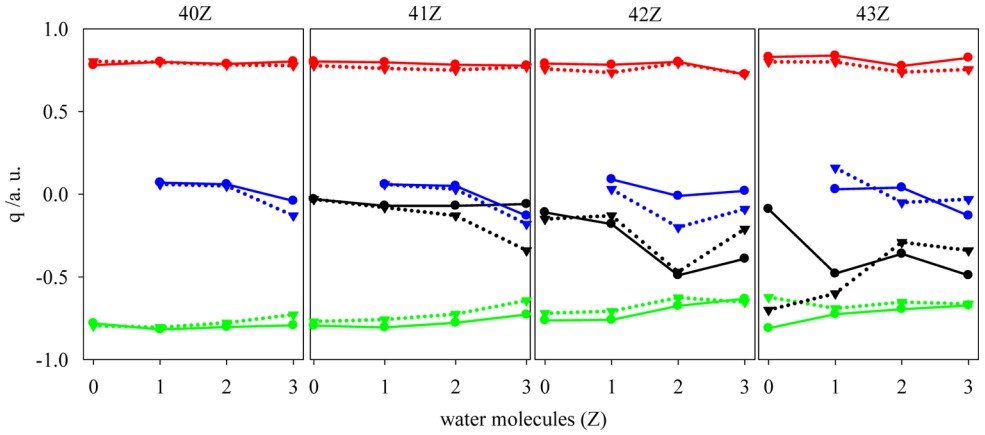

Figure 6. Evolution of the total charge, computed according ChelpG scheme at the B3LYP/6-31+G**level, over the cation (red line), the anion (green line), CO_2/SO_2 (black line), and H_2O (blue line) molecules for 4YZ clusters. Solid/dotted lines correspond to CO_2/SO_2 adsorption. Total charge over [CH] and [LAC] ions are divided by the number of IL molecules (4).

DOI: 10.1021/acs.jpcb.5b00184
J. Phys. Chem. B 2015, 119, 5546−5557

main bulk structural features through cluster optimizations, with fourth IL pairs and variable amounts (between zero and three) of CO_2/SO_2 and water molecules. Gas phase simulations have showed us that CO_2, SO_2, and water molecules interact with isolated ion through the OH group of the choline cation and the COO^- group of the [LAC] anion. Hence, these functional groups can be defined as *active sites* of the ILs. In the presence of both CO_2/SO_2 and H_2O, the OH of lactate can also be considered as an *active site*. The analysis of the binding energies shows that CO_2, SO_2, and water molecules interact stronger with the lactate anion. Although the largest binding energies of the water−lactate system point out to the water ability to hinder acid-gas absorption. However, the main interaction between both ions is formed between OH and COO^- groups of choline and lactate ions, respectively. Therefore, CO_2, SO_2, or water is forced to interact with the ILs through COO^- and OH groups located on the lactate anion. From the optimized systems, we have computed the released energy as well as the main thermodynamic variables related with acid-gas capture in the presence and absence of water, and water capture in the presence and absence of CO_2/SO_2. The obtained results point out to more favored water absorption. In fact, the water molecule is able to trigger an arrangement between [CH][LAC] ILs and acid gas molecule, which hinders CO_2/SO_2 capture in the presence of water. These effects are more dramatic for CO_2 capture. Based on the energetics of analyzed processes, [CH][LAC] would show similar preference to interact with SO_2 or water molecules, and thus, this leads SO_2 capture still being possible even with the presence of water. Similar conclusions are derived from cluster optimizations as well. We have also noted (from atomic charges) that high water amount is able to inhibit CO_2/SO_2 capture, since in the IL bulk most of the active sites would be interacting with water molecules. Our results point out that water presence has a dramatic hindering effect on CO_2/SO_2, mainly due to the IL priority to interact with water instead of the CO_2/SO_2 molecule. Moreover, as a final comment, CO_2 capture would be more affected by water presence when compared with a SO_2 rich system.

■ ASSOCIATED CONTENT

Supporting Information

Results computed at B3LYP-D2/6-31+G(d,p) level (Tables 1S−8S), Computed Binding energies for clusters 4YZ (Table 9S), AIM parameters for 4YZ clusters (Table 10S), computed atomic charges for 4YZ clusters (Table 11S), and molecular structures optimized at B3LYP-D2/6-31+G** level (Figure 1S). This material isavailable free of charge via the Internet at http://pubs.acs.org.

■ AUTHOR INFORMATION

Corresponding Authors

*E-mail: mert.atilhan@qu.edu.qa.

*E-mail: sapar@ubu.es.

Notes

The authors declare no competing financial interest.

■ ACKNOWLEDGMENTS

G.G. acknowledges the funding by Junta de Castilla y León, cofounded by European Social Fund, for a postdoctoral contract. S.A. acknowledges the funding by Ministerio de Economía y Competitividad (Spain, project CTQ2013-40476-R) and Junta de Castilla y León (Spain, project BU324U14). We also acknowledge The Foundation of Supercomputing Center of Castile and León (FCSCL, Spain), Computing and Advanced Technologies Foundation of Extremadura (CénitS, LUSITANIA Supercomputer, Spain) and Consortium of Scientific and Academic Services of Cataluña (CSUC, Spain) for providing supercomputing facilities. We also acknowledge the support of an NPRP grant (No. 6-330-2-140) from the Qatar National Research Fund (QNRF). The statements made herein are solely the responsibility of the authors.

■ REFERENCES

(1) Earle, M. J.; Seddon, K. R., Ionic Liquids: Green Solvents for the Future. In *Clean Solvents*; Abraham, M. A., Moens, L., Eds.; American Chemical Society: Washington, DC, 2002; Vol. *819*, pp 10−25;. Wilkes, J. S. A short history of ionic liquids-from molten salts to neoteric solvents. *Green Chem.* **2002**, *4*, 73−80. Rogers, R. D.; Seddon, K. R. Ionic Liquids-Solvents of the Future? *Science* **2003**, *302*, 792−793. Romanos, G. E.; Zubeir, L. F.; Likodimos, V.; Falaras, P.; Kroon, M. C.; Iliev, B.; Adamova, G.; Schubert, T. J. S. Enhanced CO_2 Capture in Binary Mixtures of 1-Alkyl-3-methylimidazolium Tricyanomethanide Ionic Liquids with Water. *J. Phys. Chem. B* **2013**, *117*, 12234−12251. Giffin, G. A.; Laszczynski, N.; Jeong, S.; Jeremias, S.; Passerini, S. Conformations and Vibrational Assignments of the (Fluorosulfonyl)(trifluoromethanesulfonyl)imide Anion in Ionic Liquids. *J. Phys. Chem. C* **2013**, *117*, 24206−24212.

(2) Lei, Z.; Dai, C.; Chen, B. Gas Solubility in Ionic Liquids. *Chem. Rev.* **2013**, *114*, 1289−1326.

(3) Bates, E. D.; Mayton, R. D.; Ntai, I.; Davis, J. H. CO_2 Capture by a Task-Specific Ionic Liquid. *J. Am. Chem. Soc.* **2002**, *124*, 926−927.

(4) Karadas, F.; Atilhan, M.; Aparicio, S. Review on the Use of Ionic Liquids (ILs) as Alternative Fluids for CO2 Capture and Natural Gas Sweetening. *Energy Fuels* **2010**, *24*, 5817−5828.

(5) Palgunadi, J.; Kang, J.-E.; Cheong, M.-S.; Kim, H.-G.; Lee, H.-J.; Kim, H.-S. Fluorine-Free Imidazolium-Based Ionic Liquids with a Phosphorous-Containing Anion as Potential CO. *Bull. Korean Chem. Soc.* **2009**, *30*, 1749−1754. Wang, C.; Luo, H.; Luo, X.; Li, H.; Dai, S. Equimolar CO_2 capture by imidazolium-based ionic liquids and superbase systems. *Green Chem.* **2010**, *12*, 2019−2023. Shiflett, M. B.; Drew, D. W.; Cantini, R. A.; Yokozeki, A. Carbon Dioxide Capture Using Ionic Liquid 1-Butyl-3-methylimidazolium Acetate. *Energy Fuels* **2010**, *24*, 5781−5789. Gurkan, B. E.; de la Fuente, J. C.; Mindrup, E. M.; Ficke, L. E.; Goodrich, B. F.; Price, E. A.; Schneider, W. F.; Brennecke, J. F. Equimolar CO_2 Absorption by Anion-Functionalized Ionic Liquids. *J. Am. Chem. Soc.* **2010**, *132*, 2116−2117. Ren, S.; Hou, Y.; Tian, S.; Chen, X.; Wu, W. What Are Functional Ionic Liquids for the Absorption of Acidic Gases? *J. Phys. Chem. B* **2013**, *117*, 2482−2486.

(6) Zhang, X.; Liu, Z.; Wang, W. Screening of ionic liquids to capture CO_2 by COSMO-RS and experiments. *AIChE J.* **2008**, *54*, 2717−2728.

(7) Liu, H.; Dai, S.; Jiang, D.-e. Solubility of Gases in a Common Ionic Liquid from Molecular Dynamics Based Free Energy Calculations. *J. Phys. Chem. B* **2014**, *118*, 2719−2725.

(8) Aparicio, S.; Atilhan, M.; Khraisheh, M.; Alcalde, R.; Fernández, J. Study on Hydroxylammonium-Based Ionic Liquids. II. Computational Analysis of CO_2 Absorption. *J. Phys. Chem. B* **2011**, *115*, 12487−12498.

(9) Gurkan, B.; Goodrich, B. F.; Mindrup, E. M.; Ficke, L. E.; Massel, M.; Seo, S.; Senftle, T. P.; Wu, H.; Glaser, M. F.; Shah, J. K.; Maginn, E. J.; Brennecke, J. F.; Schneider, W. F. Molecular Design of High Capacity, Low Viscosity, Chemically Tunable Ionic Liquids for CO_2 Capture. *J. Phys. Chem. Lett.* **2010**, *1*, 3494−3499. Yan, F.; Lartey, M.; Damodaran, K.; Albenze, E.; Thompson, R. L.; Kim, J.; Haranczyk, M.; Nulwala, H. B.; Luebke, D. R.; Smit, B. Understanding the effect of side groups in ionic liquids on carbon-capture properties: A combined experimental and theoretical effort. *Phys. Chem. Chem. Phys.* **2013**, *15*, 3264−3272.

DOI: 10.1021/acs.jpcb.5b00184
J. Phys. Chem. B 2015, 119, 5546−5557

(10) Wu, C.; Senftle, T. P.; Schneider, W. F. First-principles-guided design of ionic liquids for CO_2 capture. *Phys. Chem. Chem. Phys.* **2012**, *14*, 13163−13170. Maiti, A. Atomistic modeling toward high-efficiency carbon capture: A brief survey with a few illustrative examples. *Int. J. Quantum Chem.* **2014**, *114*, 163−175.
(11) Aparicio, S.; Atilhan, M. A Computational Study on Choline Benzoate and Choline Salicylate Ionic Liquids in the Pure State and After CO_2 Adsorption. *J. Phys. Chem. B* **2012**, *116*, 9171−9185.
(12) Shi, W.; Maginn, E. J. Atomistic Simulation of the Absorption of Carbon Dioxide and Water in the Ionic Liquid 1-*n*-Hexyl-3-methylimidazolium Bis(trifluoromethylsulfonyl)imide ([hmim][Tf_2N]. *J. Phys. Chem. B* **2008**, *112*, 2045−2055.
(13) Kohno, Y.; Ohno, H. Ionic liquid/water mixtures: From hostility to conciliation. *Chem. Commun.* **2012**, *48*, 7119−7130. Yaghini, N.; Nordstierna, L.; Martinelli, A. Effect of water on the transport properties of protic and aprotic imidazolium ionic liquids - An analysis of self-diffusivity, conductivity, and proton exchange mechanism. *Phys. Chem. Chem. Phys.* **2014**, *16*, 9266−9275. Martins, V. L.; Nicolau, B. G.; Urahata, S. M.; Ribeiro, M. C. C.; Torresi, R. M. Influence of the Water Content on the Structure and Physicochemical Properties of an Ionic Liquid and Its Li+ Mixture. *J. Phys. Chem. B* **2013**, *117*, 8782−8792.
(14) Goodrich, B. F.; de la Fuente, J. C.; Gurkan, B. E.; Lopez, Z. K.; Price, E. A.; Huang, Y.; Brennecke, J. F. Effect of Water and Temperature on Absorption of CO_2 by Amine-Functionalized Anion-Tethered Ionic Liquids. *J. Phys. Chem. B* **2011**, *115*, 9140−9150. McDonald, J.; Sykora, R.; Hixon, P.; Mirjafari, A.; Davis, J., Jr. Impact of water on CO2 capture by amino acid ionic liquids. *Environ. Chem. Lett.* **2014**, *12*, 201−208.
(15) Husson, P.; Pison, L.; Jacquemin, J.; Gomes, M. F. C. Influence of water on the carbon dioxide absorption by 1-ethyl-3-methylimidazolium bis(trifluoromethylsulfonyl)amide. *Fluid Phase Equilib.* **2010**, *294*, 98−104.
(16) Stevanovic, S.; Podgoršek, A.; Pádua, A. A. H.; Costa Gomes, M. F. Effect of Water on the Carbon Dioxide Absorption by 1-Alkyl-3-methylimidazolium Acetate Ionic Liquids. *J. Phys. Chem. B* **2012**, *116*, 14416−14425.
(17) Perez-Blanco, M. E.; Maginn, E. J. Molecular Dynamics Simulations of Carbon Dioxide and Water at an Ionic Liquid Interface. *J. Phys. Chem. B* **2011**, *115*, 10488−10499.
(18) Cui, G.; Lin, W.; Ding, F.; Luo, X.; He, X.; Li, H.; Wang, C. Highly efficient SO_2 capture by phenyl-containing azole-based ionic liquids through multiple-site interactions. *Green Chem.* **2014**, *16*, 1211−1216. Tian, S.; Hou, Y.; Wu, W.; Ren, S.; Zhang, C. Absorption of SO_2 by thermal-stable functional ionic liquids with lactate anion. *RSC Adv.* **2013**, *3*, 3572−3577. Cui, G.; Zheng, J.; Luo, X.; Lin, W.; Ding, F.; Li, H.; Wang, C. Tuning Anion-Functionalized Ionic Liquids for Improved SO_2 Capture. *Angew. Chem., Int. Ed.* **2013**, *52*, 10620−10624.
(19) Ren, S.; Hou, Y.; Wu, W.; Liu, Q.; Xiao, Y.; Chen, X. Properties of Ionic Liquids Absorbing SO_2 and the Mechanism of the Absorption. *J. Phys. Chem. B* **2010**, *114*, 2175−2179.
(20) Wu, W.; Han, B.; Gao, H.; Liu, Z.; Jiang, T.; Huang, J. Desulfurization of Flue Gas: SO_2 Absorption by an Ionic Liquid. *Angew. Chem., Int. Ed.* **2004**, *43*, 2415−2417. Huang, J.; Riisager, A.; Wasserscheid, P.; Fehrmann, R. Reversible physical absorption of SO_2 by ionic liquids. *Chem. Commun.* **2006**, 4027−4029. Yuan, X. L.; Zhang, S. J.; Lu, X. M. Hydroxyl Ammonium Ionic Liquids: Synthesis, Properties, and Solubility of SO_2. *J. Chem. Eng. Data* **2007**, *52*, 596−599. Shiflett, M. B.; Yokozeki, A. Chemical Absorption of Sulfur Dioxide in Room-Temperature Ionic Liquids. *Ind. Eng. Chem. Res.* **2009**, *49*, 1370−1377. Wick, C. D.; Chang, T.-M.; Dang, L. X. Molecular Mechanism of CO_2 and SO_2 Molecules Binding to the Air/Liquid Interface of 1-Butyl-3-methylimidazolium Tetrafluoroborate Ionic Liquid: A Molecular Dynamics Study with Polarizable Potential Models. *J. Phys. Chem. B* **2010**, *114*, 14965−14971. Yu, G.; Chen, X. SO_2 Capture by Guanidinium-Based Ionic Liquids: A Theoretical Study. *J. Phys. Chem. B* **2011**, *115*, 3466−3477. Cui, G.; Wang, C.; Zheng, J.; Guo, Y.; Luo, X.; Li, H. Highly efficient SO2 capture by dual functionalized ionic liquids through a combination of chemical and physical absorption. *Chem. Commun.* **2012**, *48*, 2633−2635. Wang, Y.; Pan, H.; Li, H.; Wang, C. Force Field of the TMGL Ionic Liquid and the Solubility of SO_2 and CO_2 in the TMGL from Molecular Dynamics Simulation. *J. Phys. Chem. B* **2007**, *111*, 10461−10467.
(21) Aparicio, S.; Atilhan, M. Water effect on CO_2 absorption for hydroxylammonium based ionic liquids: A molecular dynamics study. *Chem. Phys.* **2012**, *400*, 118−125.
(22) Shi, W.; Myers, C. R.; Luebke, D. R.; Steckel, J. A.; Sorescu, D. C. Theoretical and Experimental Studies of CO_2 and H_2 Separation Using the 1-Ethyl-3-methylimidazolium Acetate ([emim][CH3COO]) Ionic Liquid. *J. Phys. Chem. B* **2011**, *116*, 283−295. Teague, C. M.; Dai, S.; Jiang, D.-e. Computational Investigation of Reactive to Nonreactive Capture of Carbon Dioxide by Oxygen-Containing Lewis Bases. *J. Phys. Chem. A* **2010**, *114*, 11761−11767. Lourenço, T. C.; Coelho, M. F. C.; Ramalho, T. C.; van der Spoel, D.; Costa, L. T. Insights on the Solubility of CO_2 in 1-Ethyl-3-methylimidazolium Bis(trifluoromethylsulfonyl)imide from the Microscopic Point of View. *Environ. Sci. Technol.* **2013**, *47*, 7421−7429. Gu, P.; Lü, R.; Wang, S.; Lu, Y.; Liu, D. The comparative study on interactions between ionic liquid and CO_2/SO_2 by a hybrid density functional approach in the gas phase. *Comput. Theor. Chem.* **2013**, *1020*, 22−31. Sanz, V.; Alcalde, R.; Atilhan, M.; Aparicio, S. Insights from quantum chemistry into piperazine-based ionic liquids and their behavior with regard to CO2. *J. Mol. Model.* **2014**, *20*, 1−14.
(23) Klamt, A., Chapter 1 - Introduction. In *COSMO-RS*; Klamt, A., Ed.; Elsevier: Amsterdam, 2005; pp 1−9.
(24) Palomar, J.; Gonzalez-Miquel, M.; Polo, A.; Rodriguez, F. Understanding the Physical Absorption of CO_2 in Ionic Liquids Using the COSMO-RS Method. *Ind. Eng. Chem. Res.* **2011**, *50*, 3452−3463.
(25) Couling, D. J.; Bernot, R. J.; Docherty, K. M.; Dixon, J. K.; Maginn, E. J. Assessing the factors responsible for ionic liquid toxicity to aquatic organisms via quantitative structure-property relationship modeling. *Green Chem.* **2006**, *8*, 82−90.
(26) Nockemann, P.; Thijs, B.; Driesen, K.; Janssen, C. R.; Van Hecke, K.; Van Meervelt, L.; Kossmann, S.; Kirchner, B.; Binnemans, K. Choline Saccharinate and Choline Acesulfamate: Ionic Liquids with Low Toxicities. *J. Phys. Chem. B* **2007**, *111*, 5254−5263.
(27) Aparicio, S.; Atilhan, M.; Khraisheh, M.; Alcalde, R. Study on Hydroxylammonium-Based Ionic Liquids. I. Characterization. *J. Phys. Chem. B* **2011**, *115*, 12473−12486.
(28) Dong, K.; Song, Y.; Liu, X.; Cheng, W.; Yao, X.; Zhang, S. Understanding Structures and Hydrogen Bonds of Ionic Liquids at the Electronic Level. *J. Chem. Phys. B* **2012**, *116*, 1007−1017.
(29) Ober, C. A.; Gupta, R. B. pH Control of Ionic Liquids with Carbon Dioxide and Water: 1-Ethyl-3-methylimidazolium Acetate. *Ind. Eng. Chem. Res.* **2012**, *51*, 2524−2530.
(30) Murphy, L. J.; McPherson, A. M.; Robertson, K. N.; Clyburne, J. A. C. Ionic liquids and acid gas capture: water and oxygen as confounding factors. *Chem. Commun.* **2012**, *48*, 1227−1229.
(31) Becke, A. D. Density-functional exchange-energy approximation with correct asymptotic behavior. *Phys. Rev. A* **1988**, *38*, 3098−3100. Becke, A. D., Density-functional thermochemistry. III. The role of exact exchange. *J. Chem. Phys.***1993**, *98*;. Lee, C.; Yang, W.; Parr, R. G. Development of the Colle-Salvetti correlation-energy formula into a functional of the electron density. *Phys. Rev. B* **1988**, *37*, 785−789.
(32) Grimme, S. Semiempirical GGA-type density functional constructed with a long-range dispersion correction. *J. Comput. Chem.* **2006**, *27*, 1787−1799.
(33) Schwabe, T.; Grimme, S. Double-hybrid density functionals with long-range dispersion corrections: higher accuracy and extended applicability. *Phys. Chem. Chem. Phys.* **2007**, *9*, 3397−3406.
(34) Frisch, M. J.; Trucks, G. W.; Schlegel, H. B.; Scuseria, G. E.; Robb, M. A.; Cheeseman, J. R.; Scalmani, G.; Barone, V.; Mennucci, B.; Petersson, G. A.; Nakatsuji, H.; Caricato, M.; Li, X.; Hratchian, H. P.; Izmaylov, A. F.; Bloino, J.; Zheng, G.; Sonnenberg, J. L.; Hada, M.; Ehara, M.; Toyota, K.; Fukuda, R.; Hasegawa, J.; Ishida, M.; Nakajima, T.; Honda, Y.; Kitao, O.; Nakai, H.; Vreven, T.; Montgomery, J. A., Jr.; Peralta, J. E.; Ogliaro, F. o.; Bearpark, M. J.; Heyd, J.; Brothers, E. N.;

DOI: 10.1021/acs.jpcb.5b00184
J. Phys. Chem. B 2015, 119, 5546−5557

Kudin, K. N.; Staroverov, V. N.; Kobayashi, R.; Normand, J.; Raghavachari, K.; Rendell, A. P.; Burant, J. C.; Iyengar, S. S.; Tomasi, J.; Cossi, M.; Rega, N.; Millam, N. J.; Klene, M.; Knox, J. E.; Cross, J. B.; Bakken, V.; Adamo, C.; Jaramillo, J.; Gomperts, R.; Stratmann, R. E.; Yazyev, O.; Austin, A. J.; Cammi, R.; Pomelli, C.; Ochterski, J. W.; Martin, R. L.; Morokuma, K.; Zakrzewski, V. G.; Voth, G. A.; Salvador, P.; Dannenberg, J. J.; Dapprich, S.; Daniels, A. D.; Farkas, Ã. d. n.; Foresman, J. B.; Ortiz, J. V.; Cioslowski, J.; Fox, D. J. *Gaussian 09*; Gaussian, Inc.: Wallingford, CT, 2009.

(35) Soler, J. M.; Artacho, E.; Gale, J. D.; García, A.; Junquera, J.; Ordejón, P. DanielSánchez-Portal, The SIESTA method for ab initio order-N materials simulation. *J. Phys.: Condens. Matter* **2002**, *14*, 2745−2779.

(36) Perdew, J. P.; Ernzerhof, K. B. Generalized Gradient Approximation Made Simple. *Phys. Rev. Lett.* **1996**, *77*, 3865−3868.

(37) Simon, S.; Duran, M.; Dannenberg, J. J. How does basis set superposition error change the potential surfaces for hydrogen-bonded dimers? *J. Chem. Phys.* **1996**, *105*, 11024.

(38) Bader, R. F. W. *Atoms in Molecules: A Quantum Theory*; Oxford University Press: Oxford, 1990

(39) Lu, T.; Chen, F. Multiwfn: A multifunctional wavefunction analyzer. *J. Comput. Chem.* **2012**, *33*, 580−592.

(40) Breneman, C. M.; Wiberg, K. B. Determining atom-centered monopoles from molecular electrostatic potentials. The need for high sampling density in formamide conformational analysis. *J. Comput. Chem.* **1990**, *11*, 361−373.

(41) Aparicio, S.; Atilhan, M. A Computational Study on Choline Benzoate and Choline Salicylate Ionic Liquids in the Pure State and After CO_2 Adsorption. *J. Chem. Phys. B* **2012**, *116*, 9171−9185.

(42) Tsuzuki, S.; Tokuda, H.; Hayamizu, K.; Watanabe, M. Magnitude and Directionality of Interaction in Ion Pairs of Ionic Liquids: Relationship with Ionic Conductivity. *J. Phys. Chem. B* **2005**, *109*, 16474−16481.

DOI: 10.1021/acs.jpcb.5b00184
J. Phys. Chem. B 2015, 119, 5546−5557